Journal of Cancer Research and Clinical Oncology (2019) 145:2921–2936
https://doi.org/10.1007/s00432-019-03047-2

ORIGINAL ARTICLE – CANCER RESEARCH

Co-targeting PI3K/Akt and MAPK/ERK pathways leads to an enhanced antitumor effect on human hypopharyngeal squamous cell carcinoma

Xiaolin Peng[1,2] · Yao Liu[1,2] · Shan Zhu[1] · Xin Peng[1] · Hui Li[1] · Wenhui Jiao[1] · Peng Lin[2] · Zhe Zhang[1] · Yuling Qiu[1] · Meihua Jin[1] · Ran Wang[1] · Dexin Kong[1,3]

Received: 12 August 2019 / Accepted: 4 October 2019 / Published online: 16 October 2019

Abstract

Purpose The present study aims to determine whether co-targeting PI3K/Akt and MAPK/ERK pathways in human hypopharyngeal squamous cell carcinoma (HSCC) is a potential anticancer strategy.

Methods We retrospectively analyzed the clinical data of HSCC patients, and the phosphorylation status of Akt and Erk in HSCC and tumor adjacent tissues was evaluated by immunohistochemistry. MTT and colony formation assay were performed to determine the anti-proliferative effect of PI3K/mTOR inhibitor GDC-0980 and MEK inhibitor Refametinib on HSCC cell line Fadu. Wound-healing and Transwell migration assay were used to analyze the anti-migrative capability of the two drugs. The involved anti-tumor mechanism was explored by flow cytometry, qRT-PCR and western blot. The combinational anticancer effect of GDC-0980 and Refametinib was evaluated according to Chou and Talalay's method.

Results The levels of p-Akt and p-Erk were increased significantly with the progression of clinical stage of HSCC, suggesting PI3K/Akt and MAPK/ERK pathways might be associated with HSCC occurrence and progression. Furthermore, both GDC-0980 and Refametinib showed obvious antitumor effects on FaDu cells. Treatment by the two drugs arrested FaDu cell cycle progression in G1 phase, with reduction of cyclin D1 and p-Rb, in contrast to enhancement of p27. GDC-0980 inhibited FaDu cell migration and reduced metastasis related proteins including p-PKCζ, p-Integrin β1 and uPA. Combination use of GDC-0980 and Refametinib exhibited strong synergistic anti-tumor effect.

Conclusion Dual inhibition of PI3K/Akt and MAPK/ERK pathway by GDC-0980 and Refametinib might be a promising treatment strategy for HSCC patients.

Keywords Hypopharyngeal squamous cell carcinoma · PI3K/Akt · MAPK/ERK · Co-targeting · G1 phase arrest · Combination treatment

Introduction

Head and neck squamous cell carcinoma (HNSCC) is the sixth most common malignancy with an annual incidence of 600,000 worldwide (Parfenov et al. 2014; Siegel et al. 2013). HNSCC contains many different types of cancers starting in several places in head and throat, including those of oral cavity, larynx, pharynx, paranasal sinuses, etc. (Siegel et al. 2013). Hypopharyngeal squamous cell carcinoma (HSCC) is a rare cancer that represents about 4% of HNSCC but it has the highest mortality rate among the head and neck cancers (Kuo et al. 2016). The reason lies in the depth of lesion location and the slur of early symptom. And the majority of HSCC patients are diagnosed at advanced stages (Davies and Welch 2006; Kwon and Miles 2019). Standard HSCC

Xiaolin Peng and Yao Liu contributed equally to this work.

Electronic supplementary material The online version of this article (https://doi.org/10.1007/s00432-019-03047-2) contains supplementary material, which is available to authorized users.

✉ Ran Wang
wangran@tmu.edu.cn

✉ Dexin Kong
kongdexin@tmu.edu.cn

1 Tianjin Key Laboratory on Technologies Enabling Development of Clinical Therapeutics and Diagnostics, School of Pharmacy, Tianjin Medical University, 300070 Tianjin, China

2 Department of Otorhinolaryngology Head and Neck Surgery, Tianjin First Central Hospital, 300192 Tianjin, China

3 School of Medicine, Tianjin Tianshi College, Tianyuan University, 301700 Tianjin, China

therapy generally combines surgery, radiotherapy and chemotherapy. However, even with these treatments, the overall survival rate of HSCC patients remains less than 50% (Newman et al. 2015). In recent years, personalized treatment and molecular targeting anti-tumor agents have gain great achievements in oncotherapy. With the rapid development of genomics and proteomics, more and more potential therapeutic targets have been identified (Wang et al. 2015; Ren et al. 2016). Therefore, to understand the pathogenesis and develop effective therapeutic approaches for HSCC are imperative.

The phosphatidylinositol-3 kinase (PI3K) pathway is a key signal transduction pathway that mediates multiple cellular functions critical to cancer initiation, progression, and outcome, including growth, metabolism, migration, invasion, and angiogenesis (Shaw et al. 2006; Mayer and Arteaga 2016). Hyperactivation of PI3K/Akt/mTOR signaling cascades has been identified in a variety of human cancers, making the enzymes of this pathway ideal cancer targets (Thorpe et al. 2015). PI3K signaling pathway has attracted attention as promising target for HNSCC therapy, since PI3K overactivation is observed in up to 60% of HNSCC cases (Kundu and Nestor 2012; Machiels and Schmitz 2011). As reported, dual inhibition of PI3K and mTOR significantly suppressed the growth of implanted tumor in HNSCC xenograft model, further supporting PI3K as a target in HNSCC. Currently, two PI3K inhibiters, BYL719 and BKM120 are under investigation on HNSCC patients in different stages (Massacesi et al. 2016). However, the role of PI3K pathway in and the efficacy of PI3K inhibitors on HSCC are still unclear.

On the other hand, the mitogen-activated protein kinase/extracellular signal-regulated (MAPK/ERK) cascade is also important for human cancer cell growth, survival, and differentiation (De Luca et al. 2012). PI3K/Akt and MAPK/ERK pathways were reported to be co-activated in HNSCC (Bancroft et al. 2001). MAPK/ERK pathway consists a series of proteins including Ras, Raf, MEK and ERK. Therapies targeting such molecules have shown efficiency for therapy of various solid tumors such as melanoma and colon cancer (Bancroft et al. 2001; Cargnello and Roux 2011). A crosstalk was reported between the PI3K/Akt and MAPK/ERK pathways in regulating cell survival and inhibition of either pathway could result in compensatory activation of the other (Aksamitiene et al. 2012). Inhibition of both pathways has shown synergistic effect in the treatment of some cancers (Renshaw et al. 2013; Van Dort et al. 2015; Williams et al. 2012).

In this study, we first demonstrated the role of PI3K/Akt and MAPK/ERK pathways in HSCC by comparing the phosphorylation levels of Akt and ERK in HSCC tissues with those in tumor adjacent tissues. Then the anticancer effects of PI3K inhibitor GDC-0980 and MEK inhibitor Refametinib alone or in combination on HSCC were investigated.

Materials and methods

Reagents and antibodies

GDC-0980 and Refametinib were purchased from Selleck (London, ON, Canada). MTT (3-(4, 5-Dimethyl-2-thiazolyl)-2,5-diphenyl-2H-tetrazolium bromide) reagent was purchased from Amresco (Solon, OH, USA). FITC-Annexin V/PI Apoptosis Detection Kit was obtained from BD Biosciences (San Jose, CA, USA). Propidium iodide (PI) was purchased from Sigma-Aldrich (St. Louis, MO, USA). TriZol reagent was purchased from Life Technologies (Carlsbad, CA, USA). PrimeScript™ RT Master Mix Kit and Power SYBR® Premix Ex Taq™ were obtained from Takara (Tokyo, Japan). Antibodies against PI3K-p110α, phospho-PDK1 (Ser241), phospho-Akt (Ser473), Akt, phospho-mTOR (Ser2448), phospho-p70S6 K (Thr389), phospho-Erk (Thr202/Tyr204), Lamin B and β-actin were purchased from Cell Signaling Technology (Danvers, MA, USA). Antibodies against phospho-pRb (pS780), cyclin D1 and p27 were purchased from BD Biosciences Pharmingen (San Jose, CA, USA). Mouse and rabbit HRP-conjugated secondary antibodies (Cell Signaling Technology, Danvers, MA, USA) were used at 1: 2000 in non-fat milk (5% in TBST).

Patients and clinical data collection

The study was performed on 55 patients who were diagnosed as hypopharyngeal squamous cell carcinoma (HSCC) and were treated in Tianjin first central hospital of China from 2012 to 2016. The inclusion criteria were as follows: primary hypopharyngeal squamous cell carcinoma confirmed through histopathology, well-preserved specimens, complete clinical records and pathologic data, and no anti-tumor treatment before operation including radiotherapy, chemotherapy, biotherapy. The patients include 52 (94.5%) male and 3 (5.5%) female. The median age at the time of the first operation was 61 years (ranging from 41 to 83). We retrospectively analyzed the clinical data regarding age, gender, histological stage, clinical stage, T stage and node metastasis. Moreover, the phosphorylation status of Akt and Erk on HSCC was evaluated by immunohistochemistry. The procedures were approved by the institutional review board (IRB) in accordance with the ethical standards established by Tianjin first central hospital.

Immunohistochemistry analysis

The phosphorylation status of Akt and Erk was detected and evaluated as we previously described (Peng et al. 2018). The specimens were derived from surgical excision of 55 HSCC tissues and 20 adjacent non-tumor tissues. The tissues were fixed in 4% formalin for 20–24 h and embedded in paraffin. Tissue blocks were then cut into 4 μm sections, and the diagnosis of sections was reconfirmed by the pathologists. Subsequently, the sections were incubated with primary antibodies against phospho-Akt (dilution 1:50), phospho-Erk (dilution 1:200,) and anti-mouse secondary antibody (PV6000 Kit, ZSGB-BIO, CN). Immunohistochemistry images were taken using Olympus BX51 microscope and analyzed using MetaMorpheus software. Images were scored independently by three well-trained pathologists blind to the clinical data. Staining intensity was scored as four grades: 0 for negative, 1 for weak positive, 2 for moderate positive and 3 for strong positive. Staining extent (or positive frequency) was also scored as four grades: 0 for absence of staining (< 1% cells), 1 for focally staining (< 10% cells), 2 for variably staining (10% to 50% cells), and 3 for staining of more than 50% cells. Composite scores were calculated by multiplying the intensity score by the staining extent score. Statistically, composite scores ≥ 4 were considered as positive, and scores < 4 were defined as negative.

Cell culture

Human pharyngeal squamous FaDu cell line was purchased from the cell bank of Chinese Academy of Sciences (Shanghai, China). Cells were maintained in DMEM medium (Biological Industries, Kibbutz Beit-Haemek, Israel) supplemented with 10% fetal bovine serum (FBS), 100 μg/ml streptomycin and 100 units/ml penicillin. The cells were cultured in a humidified atmosphere environment containing 5% CO_2 at 37 °C.

Cell viability assay

Cell viability was determined using MTT assay, as described by us previously (Wang et al. 2016a, b). Briefly, 200 μl of FaDu cell suspension (4×10^4 cells/ml) was seeded in each well of a 96-well plate and treated with indicated concentrations of GDC-0980 and/or Refametinib for 48 h. Subsequently, the cells were added with 20 μl of MTT solution (5 mg/ml). After a further incubation of 4 h, the culture medium was removed, and the formazan crystals were dissolved with 150 μl of DMSO. The resulting absorbance at 490 nm was measured using a microplate reader iMark (BIO-RAD, Hercules, CA, USA).

Colony formation assay

The colony formation assay was performed as we previously described (Wang et al. 2018), with a little modification. After pre-treatment with GDC-0980 and/or Refametinib for 48 h, the assay was carried out in 60-mm dishes in which there was 4 ml of 1.8% agarose at the bottom and 3 ml of 1.8% agarose containing the drug-treated cells (1.5×10^4 cells/dish) on the top. After cells growing for 14 days, the colonies were fixed with 4% paraformaldehyde and stained with 0.5% crystal violet for 30 min. The number of colonies was counted using Image J software. At least three parallel dishes were scored for each treatment.

Flow cytometry for cell cycle distribution analysis

Cell cycle distribution was analyzed by flow cytometer as we previously described (Wang et al. 2016a, b). FaDu cells (3×10^5 cells/ml) were treated with indicated concentrations of drugs for 48 h at 37 °C. Cells were then collected, washed with ice-cold PBS and fixed with 75% ethanol overnight at 4 °C. After centrifugation, the fixed cells were resuspended in PI solution (25 μg/ml) containing 0.5% Triton X-100 and 2% RNase A, incubated in the dark for 60 min, and run on BD Accuri C6 flow cytometer (BD Biosciences, San Jose, CA, USA).

Flow cytometry for cell apoptosis analysis

Apoptosis analysis was carried out by Annexin V-FITC/PI double staining as we described previously (Wang et al. 2016a, b). FaDu cells (3×10^5 cells/ml) were treated with indicated concentrations of GDC-0980 or Refametinib in 6-well plates for 48 h. After incubation, the cells were then trypsinized and resuspended in 100 μl of binding buffer, followed by incubation with Annexin V-FITC/PI solution for 15 min in the dark at room temperature. The proportion of apoptotic cells was detected using BD Accuri C6 flow cytometer (BD Biosciences, San Jose, CA, USA).

Wound-healing assay

Wound-healing assay was employed to evaluate cell migration ability as we described previously (Wang et al. 2018). Briefly, the FaDu cells (3×10^5 cells/ml) were seeded in 24-well plates and grown until confluent state, and then the cells were scratched by sterile tips. To remove debris, the cell monolayer was rinsed twice with PBS. Fresh culture medium was added with indicated concentrations of GDC-0980 or Refametinib. Twenty four hours later, the mean width of each scratch was measured using Image Pro Plus.

Transwell migration assay

Transwell chambers with 8 µm pores (Costar; Corning, New York, NY, USA) were used to perform the migration assays as reported by us previously (Wang et al. 2018). The cells (2×10^5 cells/ml) treated with GDC-0980 were seeded into the upper chamber which contained 200 µl of serum-free medium, and the lower chamber was filled with 650 µl of medium containing 10% FBS. The chambers were maintained at 37 °C, 5% CO_2 for 48 h. Afterward, the unmigrated cells were removed by cotton swabs and the inserts were then fixed in 95% ethyl for 1 h and stained with 1% eosin for 30 min. Photographs were captured and the migrated cells were counted in at least 3 random fields.

Quantitative real-time PCR (qRT-PCR)

Total RNA was extracted from FaDu cells using TriZol reagent according to the manufacturer's instructions and quantified by a Nanodrop spectrophotometer (Thermo Fisher Scientific, Waltham, MA, USA). Quantitative RT-PCR was then performed as we previously described (Zhou et al. 2016). Briefly, using PrimeScriptTM RT master mix kit, 500 ng of total RNA was reverse-transcribed into cDNA. The PCR reaction was then carried out in a system of 20 µl volume containing 1 µl of cDNA, 0.4 µl of former primer and reverse primer, 8.2 µl RNase Free Water and 10 µl of 2 × Power SYBR® Premix Ex Taq™, using a CFX96™ Real-Time PCR Detection System (BIO-RAD, Hercules, CA, USA). The relative gene expression levels were quantified using the comparative Ct (ΔΔCt) method.

Western blot analysis

Western blot analysis was performed as described in our previous report (Wang et al. 2016a, b). After incubation with indicated drugs for 24 h, the cells were collected and lysed using RIPA lysis buffer (Roche Diagnostics, Basel, Switzerland). The nuclear lysates were prepared using NE-PER Nuclear and Cytoplasmic Extraction Kit (Thermo Fisher Scientific, Waltham, MA, USA). Cell lysates with equal amount of protein were subjected to 10% SDS- PAGE and transferred onto PVDF membranes. Membranes were then hybridized with primary antibodies, followed by incubation with HRP-conjugated secondary antibodies at room temperature for 1 h. The resulting protein bands were visualized with ECL system and digitalized by scanning.

Synergism assay

The combinational anticancer effect of GDC-0980 and Refametinib on FaDu cells was evaluated as reported by the isobologram and Fa-CI plot based on Chou and Talalay's method (Zhou et al. 2017). Briefly, FaDu cells seeded in a 96-well plate were exposed to GDC-0980 and Refametinib at three constant ratios ($IC_{50\ GDC\text{-}0980}$:$IC_{50\ Refametinib}$, $0.5\times IC_{50\ GDC\text{-}0980}$:$IC_{50\ Refametinib}$, $2\times IC_{50\ GDC\text{-}0980}$:$IC_{50\ Refametinib}$) for 48 h. The cell viability was determined using MTT assay. The combination index (CI) was calculated according to Chou and Talalay's method using the CalcuSyn software. CI < 1, CI = 1 and CI > 1 indicates synergism, additivity and antagonism, respectively.

Statistical analysis

Quantitative results were analyzed by two-tailed unpaired Student's *t* test, representative of at least three independent experiments. $p<0.05$ was considered statistically significant. All statistical analyses were performed using the GraphPad Prism 5.0 (San Diego, CA, USA). The differences were analyzed by χ^2 or Fisher exact test, when applicable. We explored the correlation between expression of p-Akt and p-Erk through Pearson R test.

Results

The phosphorylation of Akt and Erk is up-regulated in HSCC tissues and positively correlated with tumor stages

It has been reported that over-activation of PI3K/Akt and/or MAPK/ERK signaling are frequent events in human cancers (Martini et al. 2013; Cargnello and Roux 2011). To investigate the role of PI3K/Akt and MAPK/ERK pathways in the occurrence and progression of HSCC, we examined the phosphorylation status of Akt and Erk in 55 HSCC tissues and 20 normal adjacent hypopharyngeal tissues. The phosphorylation level of Akt was significantly higher in tumor tissues (54.5%) compared to normal tissues (10.0%) ($p\le0.05$) (Table 1, Fig. 1a–c). Similar result was found in

Table 1 Expression patterns of p-Akt in hypopharyngeal squamous cell carcinoma (HSCC) and adjacent non-tumor tissues

Group	No.	p-Akt expression		Positive rate (%)	χ^2	*p* value
		Positive	Negative			
Normal tissues	20	2	18	10.0	10.146	0.001
HSCC tissues	55	30	25	54.5		

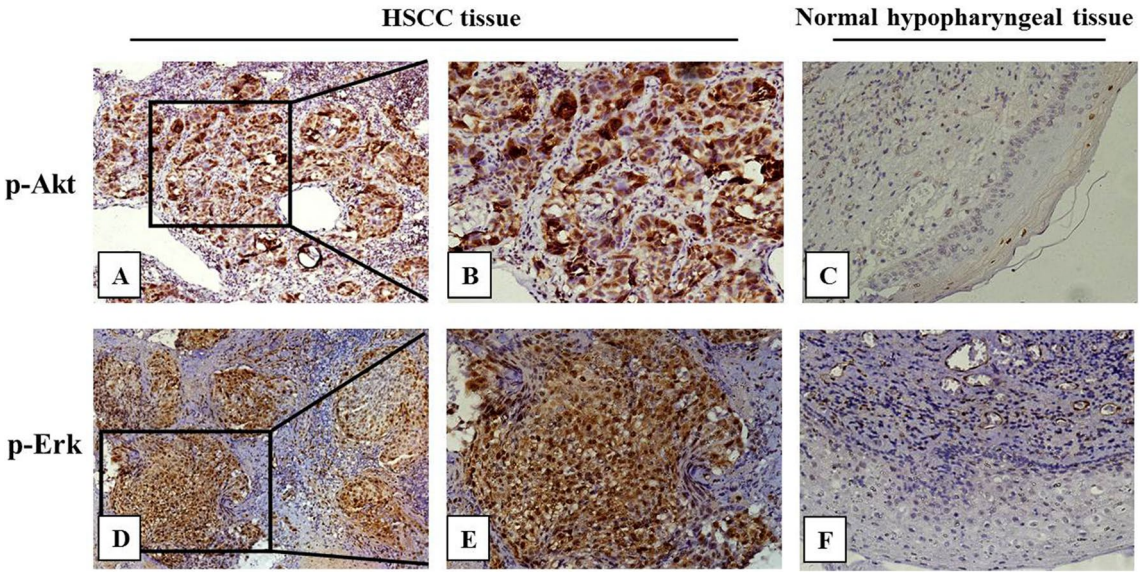

Fig. 1 Immunohistochemical analysis of p-Akt and p-Erk in HSCC tissues and adjacent non-tumor tissues. Level of p-Akt in HSCC tissues (**a**×100; **b**×200); Level of p-Akt in non-tumor tissues (**c**×200); Level of p-Erk in HSCC tissues (**d**×100; **e**×200); Level of p-Erk in non-tumor tissues (**f**×200)

Table 2 Expression patterns of p-Erk in hypopharyngeal squamous cell carcinoma (HSCC) and adjacent non-tumor tissues

Group	No.	p-Erk expression		Positive rate (%)	χ^2	*p* value
		Positive	Negative			
Normal tissues	20	5	15	25.0	9.923	0.002
HSCC tissues	55	38	17	69.1		

Table 3 Correlation analysis between p-Akt and p-Erk expression

		p-Erk expression	
		Positive	Negative
p-Akt expression	Positive	24	6
	Negative	14	11

$R = 0.259$, $p = 0.057$

the phosphorylation status of Erk, which was higher in tumor tissues (69.1%) than in normal tissues (25.0%) ($p \leq 0.05$) (Table 2, Fig. 1d–f). The correlation coefficients between the two factors were analyzed using Pearson R tests, and no statistical correlation was observed between p-Akt and p-Erk (Table 3). Additionally, we analyzed p-Akt and p-Erk in patients with different stages and tumor pathologic features (Tables 4 and 5). Among 55 tumor tissues, 75% (24/32) of T3-T4 stage tumors showed membrane staining of p-Akt, but interestingly, in 23 patients of T1-T2 stage, detection of p-Akt was restricted to only 6 (26.1%) patients. The p-Akt was increased significantly with the progression of clinical stage ($p = 0.004$). However, no association was shown between p-Akt expression and the patients' age, gender, histological grades and node metastasis. In contrast, p-Erk was positively associated with the progression of clinical stage and cervical lymph node metastasis ($p \leq 0.05$). Whereas, p-Erk expression showed no correlation with age, gender, histological grades and T stages ($p > 0.05$). These results suggested PI3K/Akt and MAPK/ERK pathways might be critical in regulating HSCC initiation and progression.

Inhibitory effect of GDC-0980 and Refametinib on cell viability of FaDu cells

To investigate whether the suppression of PI3K/Akt and MAPK/ERK pathways can inhibit HSCC growth, we explored the respective effect of PI3K/mTOR inhibitor-GDC-0980 and MEK inhibitor- Refametinib on human hypopharyngeal cancer FaDu cells. As shown in Fig. 2a, after 48 h treatment, both GDC-0980 and Refametinib effectively reduced FaDu cells viability in a dose-dependent manner, with IC50 value as 3.387 μM and 14.54 μM, respectively. Also, the phosphorylation level of Akt and Erk in FaDu cells was dramatically decreased after GDC-0980 and Refametinib treatment (Fig. 2b).

Table 4 P-Akt expression and patient clinicopathologic characteristics

Characteristics	No.	Positive	Negative	Positive rate (%)	χ^2	*p* value
Age						
< 60	25	14	11	56.0	0.039	0.843
≥ 60	30	16	15	53.3		
Gender						
Female	3	2	1	66.7		1.000*
Male	52	28	25	53.8		
Histological grades						
High-medium differentiation	39	19	20	48.7	1.836	0.175
Poor differentiation	16	11	5	68.8		
Clinical stage						
I–II	15	3	12	20.0	8.104	0.004#
III–IV	40	27	13	67.5		
T stage						
T1–T2	23	6	17	26.1	12.913	< 0.001#
T3–T4	32	24	6	75.0		
Node metastasis						
Negative	33	19	14	57.6	0.306	0.580
Positive	22	11	11	50.0		

*Gender analysis was carried out by Fisher's exact test because the cases in female group was inadequate.
#$p \leq 0.05$

Table 5 P-Erk expression and patient clinicopathologic characteristics

Characteristics	No.	Positive	Negative	Positive rate (%)	χ^2	*p* value
Age						
< 60	25	15	10	60.0	1.774	0.183
≥ 60	30	23	7	76.7		
Gender						
Female	3	1	2	33.3		0.223*
Male	52	37	15	71.2		
Histological grades						
High-medium differentiation	39	24	15	61.5	3.581	0.058
Poor differentiation	16	14	2	87.5		
Clinical stage						
I–II	15	6	9	40.0		0.008*#
III–IV	40	32	8	80.0		
T stage						
T1–T2	23	16	7	69.6	0.004	0.949
T3–T4	32	22	10	68.8		
Node metastasis						
Negative	33	18	15	54.5	6.559	0.010#
Positive	22	20	2	90.9		

*Gender and clinical stage analyses were carried out by Fisher's exact test because the cases in such groups were inadequate. #$p \leq 0.05$

GDC-0980 and Refametinib induced cell cycle arrest at G1 phase

To understand the anticancer mechanism of GDC-0980 and Refametinib on FaDu cells, we examined whether cell cycle arrest and/or apoptosis was involved in their growth inhibitory effect. The results showed that both GDC-0980 and Refametinib significantly induced G1 phase arrest in FaDu cells, compared with control group (Fig. 3a and b). On the other hand, there was no sub-G1 population was observed

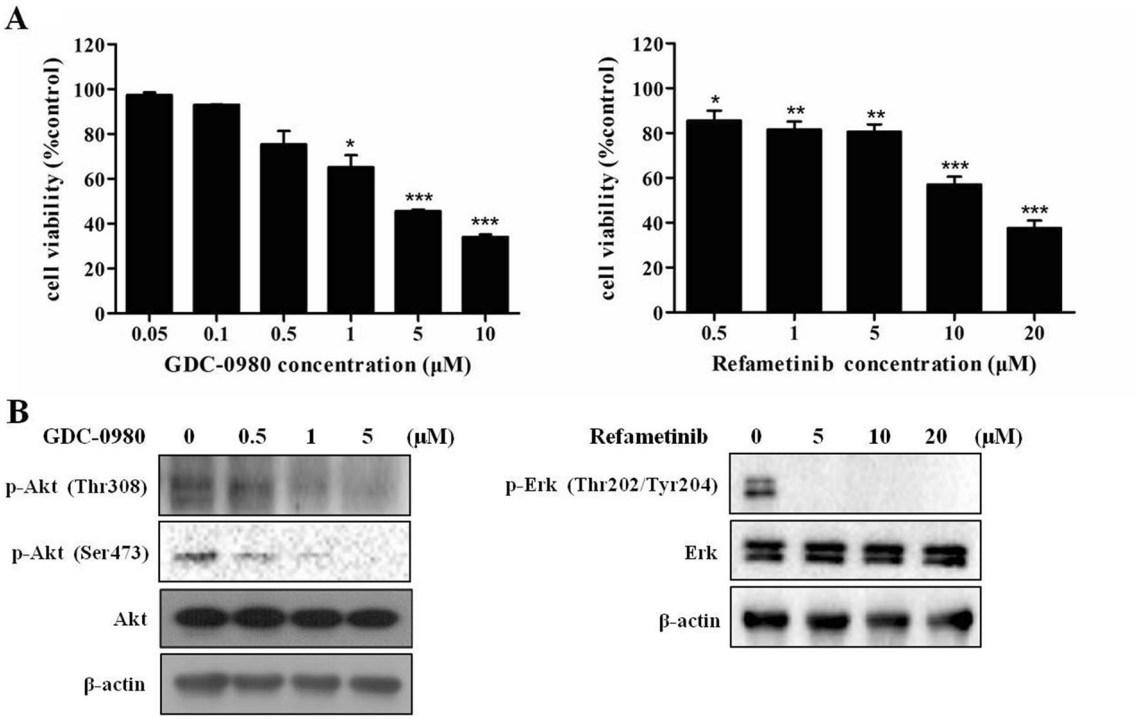

Fig. 2 Antiproliferative activities of GDC-0980 and Refametinib on FaDu cells. **a** FaDu cells were treated with indicated concentrations of GDC-0980 (**a**) and Refametinib for 48 h, respectively, and the cell viabilities were determined by MTT assay. The results are presented as mean ± SD, representative of three independent experiments ($n=3$). $^{*}p<0.05$, $^{**}p<0.01$, $^{***}p<0.001$, compared with respective control. **b** The level of p-Akt, Akt and p-Erk was determined by Western blot

in both drugs-treated groups; and the Annexin V/PI staining assay also showed no apoptotic cell population increased, suggesting that the two drugs did not induce apoptosis in FaDu cells (Fig. 3c and d). Cell cycle progression is known to be promoted by CDK (cyclin dependent kinase)-cyclin complexes and blocked by CDK inhibitors, such as p27 (Malumbres and Barbacid 2009). We next investigated the effect of GDC-0980 and Refametinib on cell cycle-related proteins involved in G1/S checkpoint to explore the potential mechanism by which the two drugs-induced G1 phase arrest. As shown in Fig. 4a, the expression of p27 increased, and the levels of cyclin D1 and phosphorylated pRb decreased dose-dependently. In addition, the RNA expression levels of p27 increased obviously after GDC-0980 and Refametinib treatment (Fig. 4b). These data indicated that the downregulation of cyclin D1 and p-pRb, and upregulation of p27 might be involved in G1 arrest induced by GDC-0980 and Refametinib.

The effect of GDC-0980 and Refametinib on the key proteins of PI3K/Akt and MAPK/ERK pathways

Since GDC-0980 is a dual PI3K/mTOR inhibitor, and PI3K/Akt/mTOR signaling plays a vital role in regulation of cell cycle progression (Powles et al. 2016; Zi et al. 2015). To further elucidate the mechanism involved in GDC-0980-induced G1 phase arrest, we investigated the effect of GDC-0980 on the key regulating proteins of PI3K/Akt pathway. As shown in Figure S1A, a dose-dependent reduction of p-PDK1, p-Akt, p-mTOR and p-p70S6 K was observed after GDC-0980 treatment. The expression of the upstream of PI3K, the catalytic subunit PI3K-p110α, was inhibited by GDC-0980 dose-dependently as well. Also, the MAPK/ERK cascades are essential in cell cycle regulation (Zhang and Liu 2002). We then determined the effect of MEK inhibitor Refametinib on the phosphorylation of Erk, the key effecter of MAPK/ERK pathway. Figure S1B showed p-Erk was remarkably reduced by Refametinib treatment.

GDC-0980 inhibited FaDu cell migration

Tumor cell detachment from the primary tumor and migration into the surrounding tissue is the initiation step in the process of tumor metastasis (Chaffer and Weinberg 2011). To test whether GDC-0980 and Refametinib can inhibit FaDu cell migration, we first performed wound-healing assay with both drugs at non-cytotoxic concentrations. As presented in Fig. 5a and b, migration distance of FaDu cells was decreased with the increasing concentrations of GDC-0980. The inhibition rate of 0.5 and 1 μM of GDC-0980

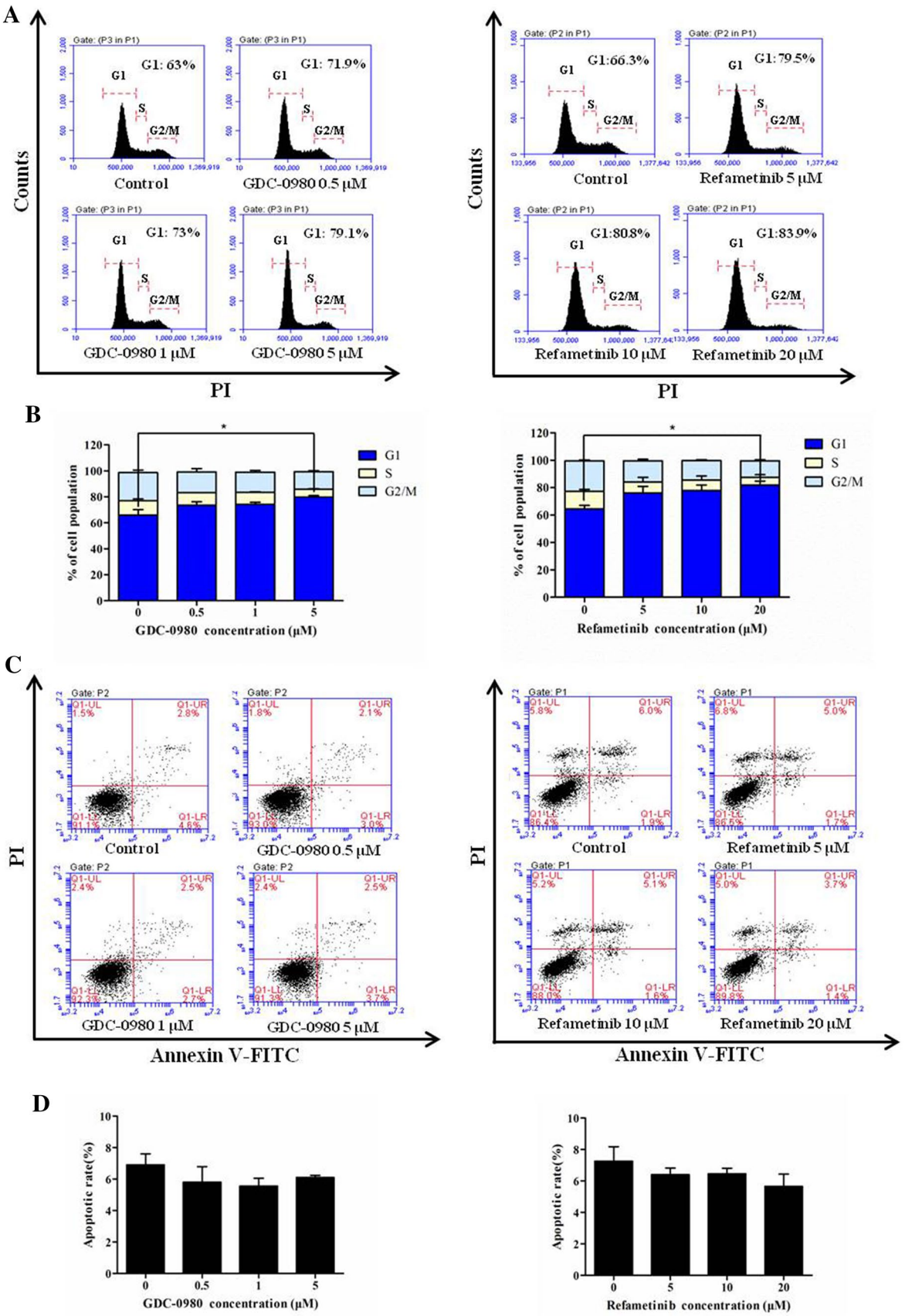
A
Counts
PI
Gate: (P3 in P1)
G1: 63%
G1: 71.9%
G1: 73%
G1: 79.1%
Control
GDC-0980 0.5 μM
GDC-0980 1 μM
GDC-0980 5 μM
Gate: (P2 in P1)
G1:66.3%
G1:79.5%
G1:80.8%
G1:83.9%
Refametinib 5 μM
Refametinib 10 μM
Refametinib 20 μM
B
% of cell population
G1
S
G2/M
GDC-0980 concentration (μM)
Refametinib concentration (μM)
C
PI
Annexin V-FITC
Gate: P2
Gate: P1
Q1-UL
Q1-UR
Q1-LL
Q1-LR
D
Apoptotic rate(%)
GDC-0980 concentration (μM)
Refametinib concentration (μM)

◂**Fig. 3** GDC-0980 and Refametinib induced cell cycle arrest at G1 phase in FaDu cells. **a** FaDu cells were incubated with indicated concentrations of GDC-0980 (0, 0.5, 1, and 5 μM) and Refametinib (0, 5, 10, and 20 μM) for 48 h, respectively. After PI staining, flow cytometry analysis was performed to determine cell cycle distribution. **b** The histograms show the percentages of cell population in G1, S, and G2/M phases. **c** The apoptosis inducing effect of GDC-0980 and Refametinib on FaDu cells. Cells were treated with the indicated concentrations of GDC-0980 and Refametinib for 48 h. The cells were harvested, double stained with Annexin V and PI, and analyzed with flow cytometry. **d** Quantification of the apoptotic cells. Data are mean ± SD, representative of three independent experiments ($n = 3$)

was approximately 34% and 53%, respectively. However, the cell migration distance was not significantly changed by Refametinib treatment (Fig. 5c and d). In addition, Transwell migration assay was carried out to further confirm the anti-migratory capacity of GDC-0980. As shown in Fig. 5e and f, GDC-0980 markedly inhibited cell migration from the upper to the lower chamber, with the inhibition rate as 61% and 84% for 0.5 and 1 μM of GDC-0980, respectively. Furthermore, to investigate the antimigratory mechanism of GDC-0980, we examined the effect of GDC-0980 on several proteins that mediate cell migration as downstream molecules of Akt. It was found that GDC-0980 inhibited the phosphorylation of PKCζ and Integrin β1, decreased the expression of uPA in a dose-dependent manner (Fig. 5g). Such results indicated inhibition of PI3K/Akt pathway and the downstream PKCζ, Integrin β1 and uPA might be related to the antimigraory effect of GDC-0980.

Synergistic effect of GDC-0980 and Refametinib on FaDu cells

To examine whether co-targeting PI3K and MEK by combination of GDC-0980 and Refametinib could show better therapeutic efficacy, we carried out a combination study using Chou and Talalay's method. Firstly, MTT assay was conducted to determine the inhibitory activities using a series of drug combinations (20%, 40%, 60%, 80%, 100% of the IC_{50} values of each drug). Three constant ratios of $0.5 \times IC_{50\ \text{GDC-0980}}$:$IC_{50\ \text{Refametinib}}$, $IC_{50\ \text{GDC-0980}}$:$IC_{50\ \text{Refametinib}}$, and $2 \times IC_{50\ \text{GDC-0980}}$:$IC_{50\ \text{Refametinib}}$ were used. All of the three drug combinations indicated greater growth inhibitory effect than either drug alone, as shown in Fig. 6a. Then combination index (CI) profiles were prepared, and the values at ED_{50}, ED_{75} and ED_{90} were calculated by CalcuSyn software and presented in Fig. 6b and Table 6. Both combinations of $2 \times IC_{50\ \text{GDC-0980}}$:$IC_{50\ \text{Refametinib}}$ and $IC_{50\ \text{GDC-0980}}$:$IC_{50\ \text{Refametinib}}$ exhibited synergistic effects ($CI < 1$), and the former combination showed stronger synergistic efficacy. Subsequently, to confirm the anti-proliferative effect of $2 \times IC_{50\ \text{GDC-0980}}$:$IC_{50\ \text{Refametinib}}$ combination, soft agar assay was carried out. Combination of GDC-0980

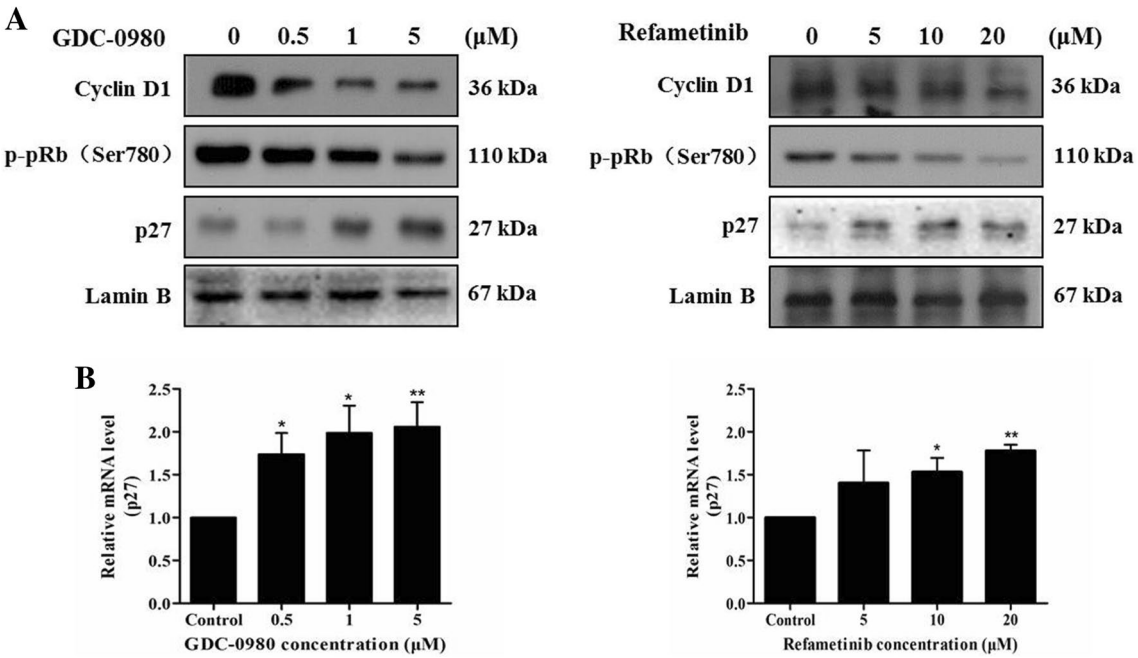

Fig. 4 GDC-0980 and Refametinib inhibited cell cycle regulatory proteins. **a** Western blot analysis of cell cycle-related proteins following GDC-0980 and Refametinib treatment. FaDu cells were exposed to indicated concentrations of GDC-0980 or Refametinib for 24 h. The expression levels of cyclin D1, p27, and the phosphorylation level of pRb in the nuclei were determined. Lamin B was used for normalization. **b** Quantitative RT-PCR analysis of p27 mRNA expression. The relative gene expression levels were quantified using the comparative Ct (ΔΔCt) method. Data are mean ± SD, representative of three independent experiments ($n = 3$). *$p < 0.05$, **$p < 0.01$, compared with respective control

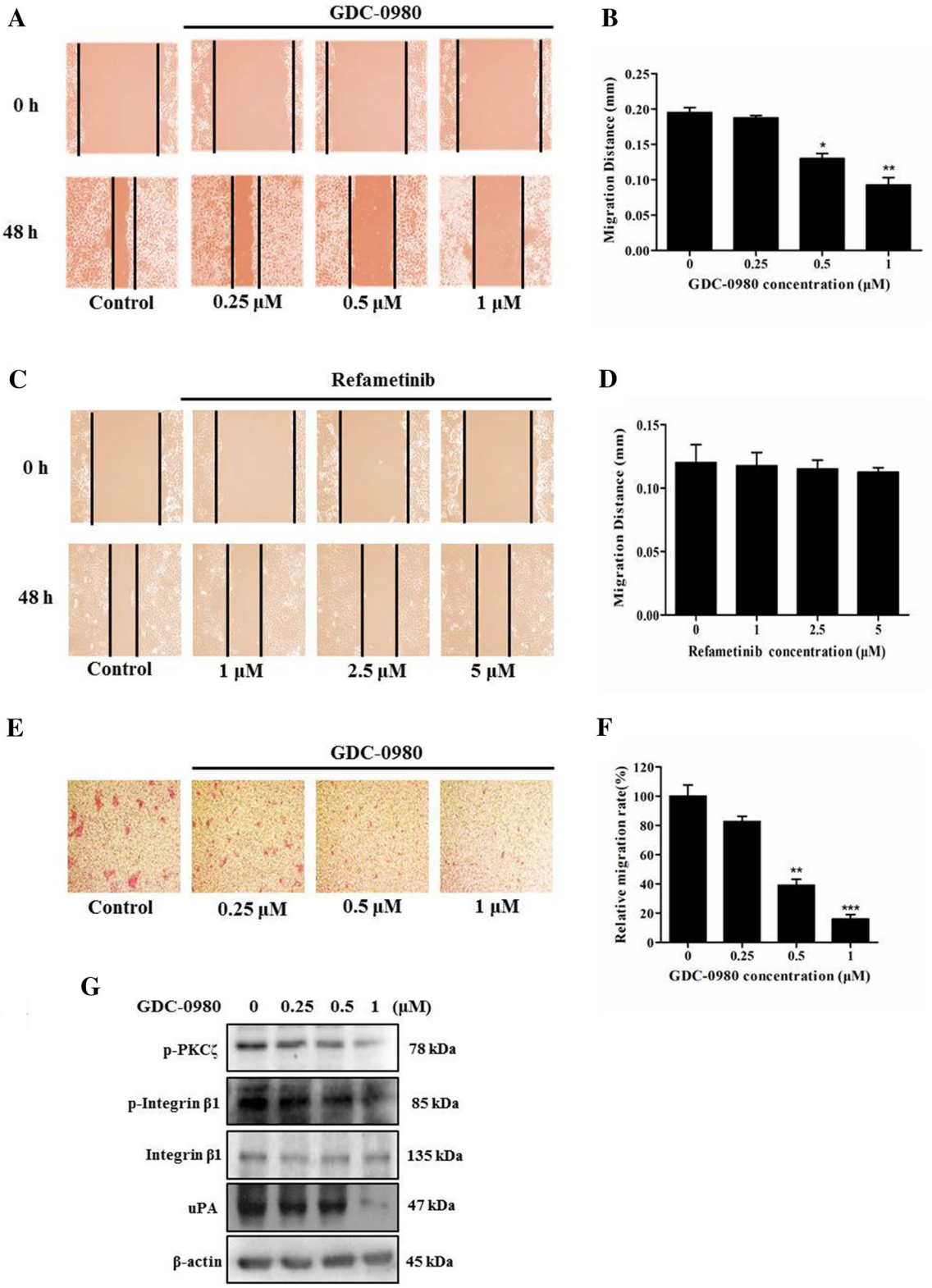
A
GDC-0980
0 h
48 h
Control
0.25 μM
0.5 μM
1 μM
B
Migration Distance (mm)
0.25
0.20
0.15
0.10
0.05
0.00
*
**
0
0.25
0.5
1
GDC-0980 concentration (μM)
C
Refametinib
0 h
48 h
Control
1 μM
2.5 μM
5 μM
D
Migration Distance (mm)
0.15
0.10
0.05
0.00
0
1
2.5
5
Refametinib concentration (μM)
E
GDC-0980
Control
0.25 μM
0.5 μM
1 μM
F
Relative migration rate(%)
120
100
80
60
40
20
0
**
***
0
0.25
0.5
1
GDC-0980 concentration (μM)
G
GDC-0980 0 0.25 0.5 1 (μM)
p-PKCζ
78 kDa
p-Integrin β1
85 kDa
Integrin β1
135 kDa
uPA
47 kDa
β-actin
45 kDa

◂**Fig. 5** GDC-0980 inhibited migration of FaDu cells. **a**–**d** FaDu cells were cultured with various concentrations of GDC-0980 and Refametinib for 48 h, respectively. **a**, **c** Images of the wound healing assay were taken at 0 h and 48 h after scratching. **b**, **d** Migration distances to the wound area following treatment with various concentrations of GDC-0980 and Refametinib. **e** Cells were treated with GDC-0980 for 48 h, and the representative pictures of migrated cells were taken. Images showed cells that migrated through the Transwell chamber membrane. **f** Percentage of cells migrated after GDC-0980 treatment compared to those without treatment. **g** The metastasis related proteins p-PKCζ, p-Integrin β1 and uPA were reduced in FaDu cells after treatment with GDC-0980 for 24 h. β-actin was used for normalization. Data are mean ± SD, representative of three independent experiments ($n = 3$). *$p < 0.05$, **$p < 0.01$, ***$p < 0.001$, compared with control

(1.356 μM) and Refametinib (2.908 μM) (the concentration of 20% of $2 \times IC_{50\ GDC\text{-}0980}$:$IC_{50\ Refametinib}$) significantly decreased the number of colonies, compared with either drug alone (Fig. 6c and d). Over all, these data demonstrated synergistic effect of combination treatment of GDC-0980 and Refametinib on FaDu cells.

Combination of GDC-0980 with Refametinib induced an enhanced G1 phase arrest compared with either drug alone

To further explore the synergistic mechanism of GDC-0980 and Refametinib, we performed cell cycle analysis with PI staining after GDC-0980/Refametinib co-treatment. The result showed the combination treatment led to a great increase of G1 phase cells, compared with GDC-0980 or Refametinib alone (Fig. 7a and b). Meanwhile, the levels of cyclin D1 and phosphorylated Rb decreased, and the expression of p27 increased (Fig. 7c). At mRNA levels, we found GDC-0980/Refametinib co-treatment significantly enhanced the expression of p27, compared with either drug alone (Fig. 7d). Interestingly, the phosphorylation status of Akt also reduced when treated with Refametinib alone (Fig. 7e). Since the Ras/ERK and PI3K/AKT pathways were reported to cross-activate each other (Mendoza et al. 2011), the inhibition of ERK phosphorylation by Refametinib might also affect PI3K/AKT pathway, therefore leading to the reduction of p-Akt. Above all, these results indicated GDC-0980/Refametinib co-treatment induced an enhanced G1 phase arrest, which might be attributed to co-targeting of both PI3K/Akt and MAPK/ERK pathways.

Discussion

It remains to be a challenge for oncologists to manage HSCC in diagnosis and treatment (Kwon and Miles 2019; Newman et al. 2015). Therefore, the identification of specific markers associated with the pathogenesis and development of HSCC and exploration of new treatment options are critical. In the present study, we examined the phosphorylation status of 2 key molecules known to be involved in carcinogesis, Akt and Erk, in 55 HPC tissue samples and 20 normal adjacent hypopharyngeal tissues. The results indicated the levels of p-Akt and p-Erk were significantly higher in HSCC tissues compared with those in non-cancerous tissues, suggesting PI3K/Akt and MAPK/ERK pathways may play an important role in the development of HSCC.

Both PI3K/Akt and MAPK/ERK pathways regulate cell survival, proliferation and motility. Besides their independent signaling that provides compensatory adjustment action, the two pathways have extensive cross-talk to regulate each other's activity positively or negatively (Mendoza et al. 2011; Steelman et al. 2011). Since the interaction between the two pathways in HSCC has not been reported yet, we analyzed the relevance of p-Akt and p-Erk in HSCC tissues. The results showed a p value of 0.057, which is very close to that (0.05) with statistical difference. Hence, we think we can not completely exclude the association between the two signaling pathways in HSCC. To support this hypothesis, further investigation with a larger sample size is needed. Furthermore, we found the amounts of p-Akt and p-Erk were correlated with clinical stage. Elevated levels of p-Akt and p-Erk were found in late stage of HSCC, suggesting the activitation of the two pathways might be associated with poor prognosis in cancer patients. Dan et al. (2010) demonstrated that the levels of phosphorylated Akt at S473 correlate to sensitivities of cancer cells to the PI3K inhibitors by use of a panel of 39 human cancer cell lines (JFCR39), they also used immunohistochemical method to confirm that the phosphorylated Akt levels correlate to the in vivo efficacy of PI3K inhibiter ZSTK474 (Isoyama et al. 2012). On the other hand, it was reported that relapsed neuroblastomas harboring hyperactivated ERK signaling was sensitive to MEK inhibition therapy (Eleveld et al. 2015). As the enhanced expression of signaling pathways could be associated with altered sensitivity to targeted therapy compared to patients that do not exhibit increased expression (McCubrey et al. 2008; Fedorov et al. 2007), inhibition of PI3K, Akt, mTOR, Raf or MEK, may be useful in HSCC treatment.

To verify our hypothesis, we determined the therapeutic efficacy of a dual PI3K/mTOR GDC-0980, and a MEK1/MEK2 inhibitor Refametinib against hypopharyngeal cancer FaDu cells in vitro. As expected, either GDC-0980 or Refametinib alone significantly decreased FaDu cell viability, with IC50 of 3.39 μM and 14.54 μM, respectively. The underlying mechanism involved G1 phase cell cycle arrest, but no apoptosis. To explore the mechanism for causing G1 phase arrest, we examined several cell cycle regulators that control G1-S transition, including cyclin D1, pRb and p27. In G1/S cell cycle checkpoint, cyclin D1 binds and activates CDK4, and then the resulting cyclin

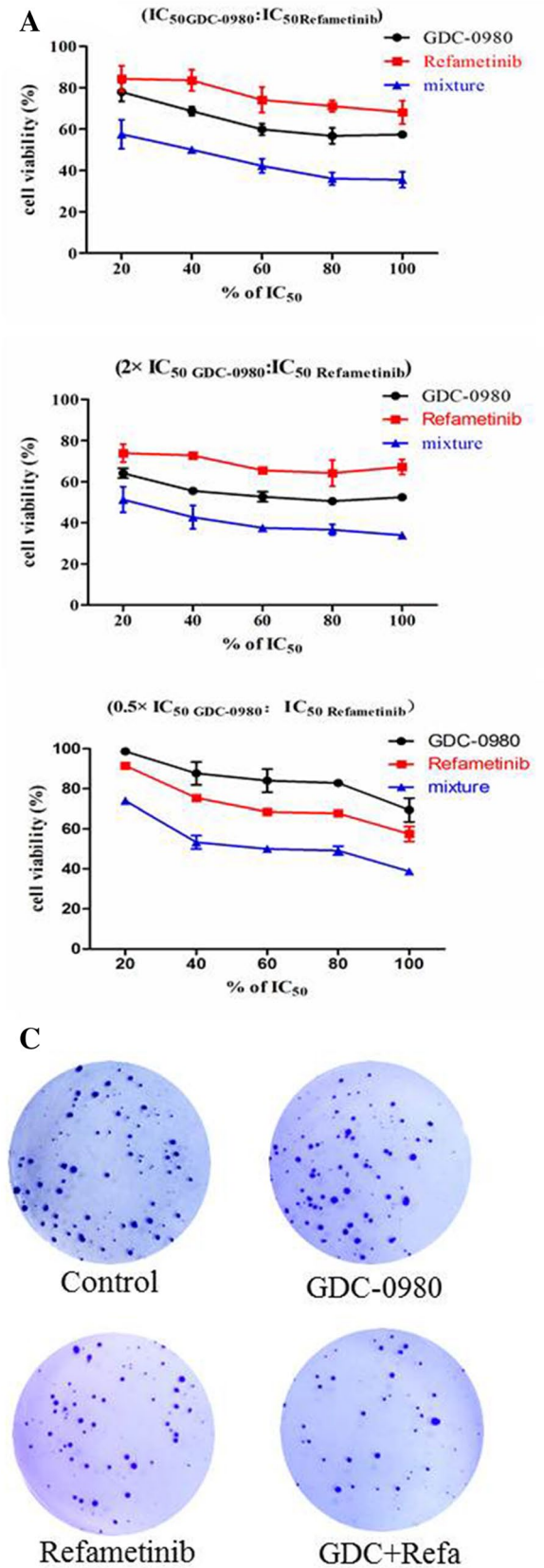
A
(IC50GDC-0980:IC50Refametinib)
GDC-0980
Refametinib
mixture
cell viability (%)
% of IC50
(2× IC50 GDC-0980:IC50 Refametinib)
(0.5× IC50 GDC-0980: IC50 Refametinib)
B
(IC50 GDC-0980:IC50 Refametinib)
(2×IC50 GDC-0980:IC50 Refametinib)
(0.5×IC50 GDC-0980:IC50 Refametinib)
Combination index(CI)
Fraction affected (Fa)
C
Control
GDC-0980
Refametinib
GDC+Refa
D
Number of colonies (% of control)
0
GDC
Refa
GDC+Refa

◂**Fig. 6** GDC-0980 and Refametinib synergized to inhibit FaDu cell proliferation. **a** FaDu cells were incubated with GDC-0980 and/or Refametinib for 48 h. Three fixed ratios of $IC_{50\ GDC}$:$IC_{50\ Refa}$, $2\times IC_{50\ GDC}$:$IC_{50\ Refa}$, and $0.5\times IC_{50\ GDC}$:$IC_{50\ Refa}$ were used to assess the combinational effect. Cell viability after different treatments was determined by MTT assay. Data are mean ± SD, representative of three independent experiments. **b** Combinational effect was analyzed using CalcuSyn software and the resulting CI-Fa plots are shown (right). The horizontal line of CI = 1, representing additivity, is indicated. Values of drug combinations below the horizontal line indicate synergism. *CI* combination index, *Fa* fraction affected. **c** The cells were treated with GDC (1.356 μM) and/or Refa (2.908 μM) for 48 h, then grown in soft agar at 37 °C for 14 days. The colonies were observed and counted under a microscope. **d** Quantification results from the data of colony formation assay. The results are mean ± SD, representative of three independent experiments ($n = 3$). $^{**}p < 0.01$, compared with control. *GDC* GDC-0980, *Refa* Refametinib

Table 6 Combination indexes (CI) for GDC-0980 and Refametinib

Drug or drug combination	*r*	CI values		
		ED_{50}	ED_{75}	ED_{90}
GDC-0980	0.979	–	–	–
Refametinib	0.938	–	–	–
GDC + Refametinib ($0.5\times IC_{50}$:IC_{50})	0.958	1.393	2.361	4.127
GDC + Refametinib (IC_{50}:IC_{50})	0.987	0.367	0.415	0.471
GDC + Refametinib ($2\times IC_{50}$:IC_{50})	0.992	0.230	0.095	0.039

D1-CDK4 complex targets pRb via phosphorylation, so that E2F is released and activated to promote cell cycle progression through G1 phase (Fedorov et al. 2007). On the other hand, the activity of cyclin D1-CDK4 complex is negatively regulated by CDK inhibitor p27 (Malumbres and Barbacid 2009). Treatment with either GDC-0980 or Refametinib led to the upregulation of p27, downregulation of cyclin D1, and the decreased phosphorylation of pRb. Consistant with the western blot result, the RNA level of p27 was also enhanced after drug treatment. Therefore, the downregulation of CDK4-cyclin D1 complex and upregulation of p27 might lead to blockade of cell cycle, which could contribute to the anticancer effect of the two drugs.

As reported, both PI3K/Akt and MAPK/ERK pathways are responsible for the regulation of cell cycle progression (Zhang and Liu 2002; Liang and Slingerland 2003 and TSC2, leading to the reduction of p27, inactivation of GSK3-β, leading to increased cyclin D1/Rb/E2F (Liang and Slingerland 2003). In MAPK/ERK pathway, the phosphorylation of ERK results in the activation of cyclin D1-CDK4/6 complex, which phosphorylates pRb and further promotes G1-S switch (Zhang and Liu 2002). Here, we found GDC-0980 remarkably suppressed the key regulators in PI3K/Akt pathway, such as the phosphorylation of PDK1, Akt, mTOR, p70S6 K, as well as the expression of PI3K-p110α. Meanwhile, Refametinib exhibited strong inhibition of ERK phosphorylation. Therefore, the effect of inducing G1 arrest by GDC-0980 and Refametinib could be attributed to the inhibition of PI3K/Akt and MAPK/ERK pathway, respectively.

As poor survival rate of HSCC is partly due to the development of distant metastasis (Wycliffe et al. 2007), discovery of innovative pharmacotherapies to control HSCC metastasis is of great importance. We next explored the effect of GDC-0980 and Refametinib on FaDu cell migration. A strong inhibition against FaDu migration was observed in GDC-0980 treated cells, but not in those treated with Refametinib. To further investigate the anti-migration mechanism of GDC-0980, we detected effect of GDC-0980 on p-PKCζ, p-Integrinβ1 as well as uPA, which are all downstream effectors of PI3K/Akt pathway. Protein kinase C (PKC) family plays pleiotropic roles in cell polarity, migration, and adhesion (Hirai and Chida 2003). It was reported that PKCζ was regulated by PI3K/Akt in human non-small cell lung cancer and breast cancer (Sun et al. 2005; Liu et al. 2009). Integrinβ1 and uPA also mediate cell migration and angiogenesis (Wang et al. 2013; Dutta et al. 2014). Our results suggested that GDC-0980 might attenuate migration of FaDu cells via inhibiting p-PKCζ, p-Integrin β1 and uPA.

Studies have suggested that a link between PI3K/Akt and MAPK/ERK pathways might give rise to redundancy in regulating cell survival. Thus, the use of combination therapy by co-targeting the molecules of both pathways may be more sufficient to treat tumor (Van Dort et al. 2015). Therefore, we analyzed the anti-tumor effiency with the joint use GDC-0980 and Refametinib. The two drugs showed a strong synergistic suppressive effect on FaDu cell viability, with an enhanced G1 phase arrest.

In conclusion, we verified PI3K/Akt and MAPK/ERK signaling pathways were activated in most HSCC tissues. PI3K/mTOR inhibitor GDC-0980 and MEK inhibitor Refametinib, exhibited antitumor activity on HSCC FaDu cells through inhibiting cell proliferation and arresting cell cycle at G1 phase. GDC-0980 could attenuate the migration of FaDu cells via inhibiting the activity of PKCζ, Integrin β1 and uPA. In addition, a significant synergy was observed when GDC-0980 combined with Refametinib in suppressing FaDu cells viability. Therefore, our research suggests that co-targeting multiple signaling nodes of the PI3K pathway and MAPK pathway might offer potential therapeutic benefits and provide a promising therapeutic approach for HSCC therapy.

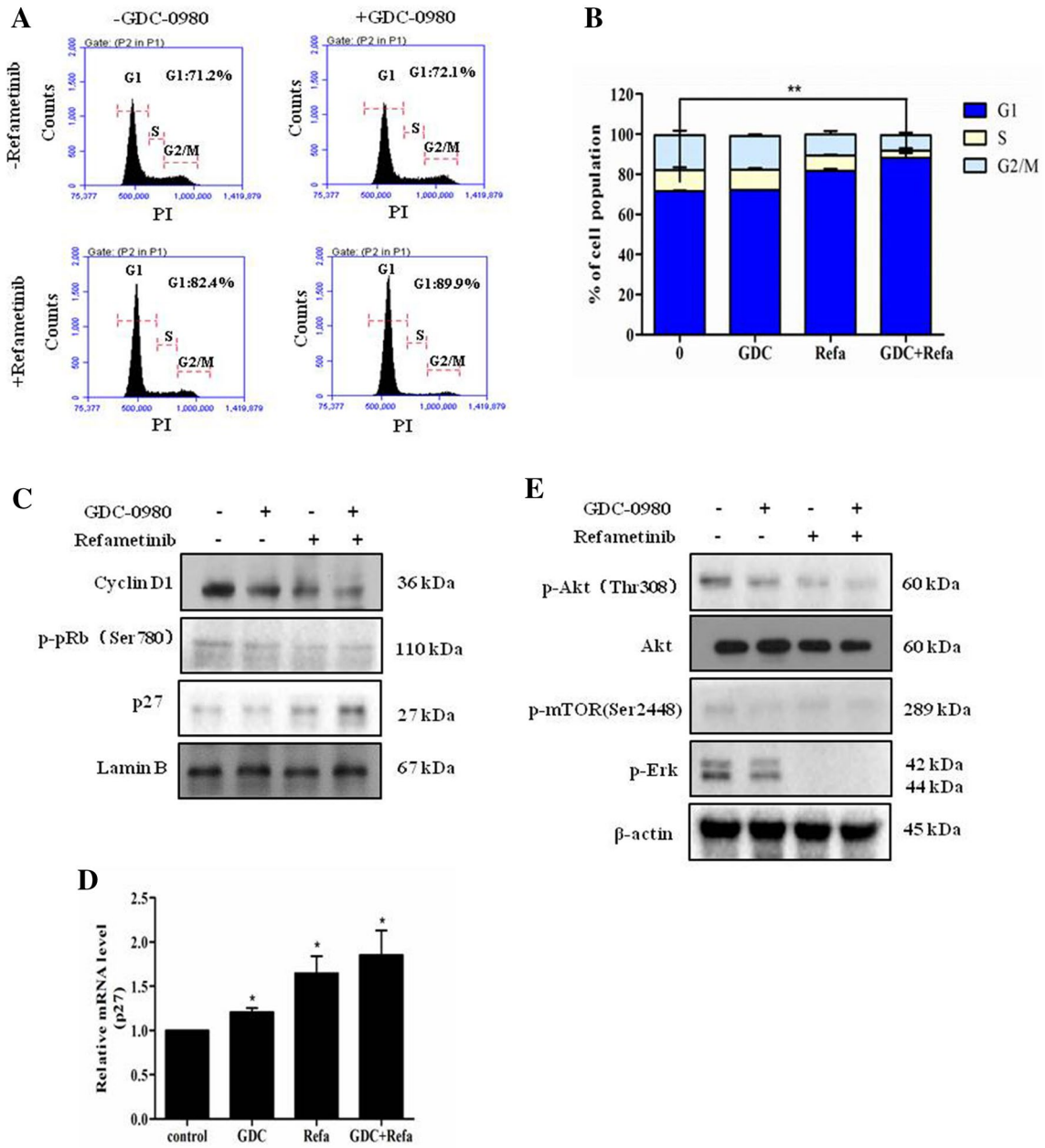

Fig. 7 Combination treatment with GDC-0980 and Refametinib induced an enhanced cell cycle arrest in FaDu cells. **a** FaDu cells exposed to GDC-0980 (1.356 μM) and/or Refametinib (2.908 μM) for 48 h, were stained with PI solution and analyzed using flow cytometer. **b** The histograms show the percentages of cell population in G1, S, and G2/M phases. **c**–**e** After treatment with GDC-0980 (1.356 μM) and/or Refametinib (2.908 μM) for 24 h, **c** the indicated cell cycle-related proteins were detected by Western blot. Lamin B was used for normalization. **d** p27 mRNA expression was examined by qRT-PCR. **e** the indicated proteins in PI3K/Akt and MAPK/ERK pathways were determined by Western blot. β-actin was used for normalization. Data are mean ± SD, representative of three independent experiments ($n = 3$). $^*p < 0.05$, compared with control. *GDC* GDC-0980, *Refa* Refametinib

Acknowledgements The work was supported by grant from National Natural Science Foundation of China (81673464, 81373441), the Grant for Major Project of Tianjin for New Drug Development (17ZXXYSY00050), and the Grant from Natural Science Foundation of Tianjin-Science and Technology (15JCYBJC27500).

Author contributions XP, YL and SZ performed the experiments. XP, HL and WJ analyzed the data. ZZ, YQ and MJ prepared the figures. YL, XP and RW wrote the main manuscript. DK revised the manuscript. PL, RW and DK designed the experiments. All authors reviewed the manuscript.

Compliance with ethical standards

Conflict of interest The authors declare that there are no conflicts of interest.

Ethical approval All procedures performed in studies involving human participants were in accordance with the ethical standards of the institutional research committee and with the 1964 Helsinki declaration and its later amendments or comparable ethical standards.

References

Aksamitiene E, Kiyatkin A, Kholodenko BN (2012) Cross-talk between mitogenic Ras/MAPK and survival PI3K/Akt pathways: a fine balance. Biochem Soc Trans 40:139–146

Bancroft CC, Chen Z, Dong G et al (2001) Coexpression of proangiogenic factors IL-8 and VEGF by human head and neck squamous cell carcinoma involves coactivation by MEK-MAPK and IKK-NF-kappaB signal pathways. Clin Cancer Res 7:435–442

Cargnello M, Roux PP (2011) Activation and function of the MAPKs and their substrates, the MAPK-activated protein kinases. Microbiol Mol Biol Rev 75:50–83

Chaffer CL, Weinberg RA (2011) A perspective on cancer cell metastasis. Science 331:1559–1564

Dan S, Okamura M, Seki M (2010) Correlating phosphatidylinositol 3-kinase inhibitor efficacy with signaling pathway status: in silico and biological evaluations. Cancer Res 70:4982–4994

Davies L, Welch HG (2006) Epidemiology of head and neck cancer in the United States. Otolaryngol Head Neck Surg 135:451–457

De Luca A, Maiello MR, D'Alessio A et al (2012) The RAS/RAF/MEK/ERK and the PI3K/AKT signalling pathways: role in cancer pathogenesis and implications for therapeutic approaches. Expert Opin Ther Targets 16:S17–S27

Dutta S, Bandyopadhyay C, Bottero V et al (2014) Angiogenin interacts with the plasminogen activation system at the cell surface of breast cancer cells to regulate plasmin formation and cell migration. Mol Oncology 8:483–507

Eleveld TF, Oldridge DA, Bernard V et al (2015) Relapsed neuroblastomas show frequent RAS-MAPK pathway mutations. Nat Genet 47:864–871

Fedorov SN, Shubina LK, Bode AM et al (2007) Dactylone inhibits epidermal growth factor-induced transformation and phenotype expression of human cancer cells and induces G1-S arrest and apoptosis. Cancer Res 67:5914–5920

Hirai T, Chida K (2003) Protein kinase Czeta (PKCzeta): activation mechanisms and cellular functions. J Biochem 133:1–7

Isoyama S, Yoshimi H, Dan S et al (2012) Development of an immunohistochemical protein quantification system in conjunction with tissue microarray technology for identifying predictive biomarkers for phosphatidylinositol 3-kinase inhibitors. Biol Pharm Bull 35:1607–1613

Kundu SK, Nestor M (2012) Targeted therapy in head and neck cancer. Tumour Biol 33:707–721

Kuo P, Sosa JA, Burtness BA et al (2016) Treatment trends and survival effects of chemotherapy for hypopharyngeal cancer: analysis of the national cancer data base. Cancer 122:1853–1860

Kwon DI, Miles BA (2019) Education Committee of the American Head and Neck Society (AHNS). Hypopharyngeal carcinoma: do you know your guidelines? Head Neck 41:569–576

Liang J, Slingerland JM (2003) Multiple roles of the PI3K/PKB (Akt) pathway in cell cycle progression. Cell Cycle 2:339–345

Liu Y, Wang B, Wang J et al (2009) Down-regulation of PKCzeta expression inhibits chemotaxis signal transduction in human lung cancer cells. Lung Cancer 63:210–218

Machiels JP, Schmitz S (2011) New advances in targeted therapies for squamous cell carcinoma of the head and neck. Anticancer Drugs 22:626–633

Malumbres M, Barbacid M (2009) Cell cycle, CDKs and cancer: a changing paradigm. Nat Rev Cancer 9:153–166

Martini M, Ciraolo E, Gulluni F et al (2013) Targeting PI3K in cancer: any good news? Front Oncol 3:108

Massacesi C, Di Tomaso E, Urban P et al (2016) PI3K inhibitors as new cancer therapeutics: implications for clinical trial design. Onco Targets Ther 9:203–210

Mayer IA, Arteaga CL (2016) The PI3K/AKT pathway as a target for cancer treatment. Ann Rev Med 67:11–28

McCubrey JA, Steelman LS, Abrams SL et al (2008) Targeting survival cascades induced by activation of Raf/Raf/MEK/ERK, PI3K/PTEN/Akt/mTOR and Jak/STAT pathways for effective leukemia therapy. Leukemia 22:708–722

Mendoza MC, Er EE, Blenis J (2011) The Ras-ERK and PI3K-mTOR pathways: crosstalk and compensation. Trends Biochem Sci 36:320–328

Newman JR, Connolly TM, Illing EA et al (2015) Survival trends in Hypopharyngeal cancer: a population based review. Laryngoscope 125:6249

Parfenov M, Pedamallu CS, Gehlenborg N et al (2014) Characterization of HPV and host genome interactions in primary head and neck cancers. Proc Natl Acad Sci USA 111:15544–15549

Peng X, Liu Y, Peng X et al (2018) Clinical features and the molecular biomarkers of olfactory neuroblastoma. Pathol Res Pract 214:1123–1129

Powles T, Lackner MR, Oudard S et al (2016) Randomized open-label phase II trial of apitolisib (GDC-0980), a novel inhibitor of the PI3K/mammalian target of rapamycin pathway, versus everolimus in patients with metastatic renal cell carcinoma. J Clin Oncol 34:1660–1668

Ren H, Guo H, Thakur A et al (2016) Blockade efficacy of MEK/ERK-dependent autophagy enhances PI3K/Akt inhibitor NVP-BKM120′s therapeutic effectiveness in lung cancer cells. Oncotarget 7:67277–67287

Renshaw J, Taylor KR, Bishop R et al (2013) Dual blockade of the PI3K/AKT/mTOR (AZD8055) and RAS/MEK/ERK (AZD6244) pathways synergistically inhibits rhabdomyosarcoma cell growth in vitro and in vivo. Clin Cancer Res 19:5940–5951

Shaw RJ, Cantley LC (2006) Ras, PI(3)K and mTOR signalling controls tumour cell growth. Nature 441:424–430

Siegel R, Naishadham D, Jemal A (2013) Cancer statistics. CA Cancer J Clin 63:11–30

Steelman LS, Chappell WH, Abrams SL et al (2011) Roles ofthe Raf/MEK/ERK and PI3K/PTEN/Akt/mTOR pathways in controlling growth and sensitivity to therapy-implications for cancer and aging. Aging (Albany NY) 3:192–222

Sun R, Gao P, Chen L et al (2005) Protein kinase C zeta is required for epidermal growth factor-induced chemotaxis of human breast cancer cells. Cancer Res 65:1433–1441

Thorpe LM, Yuzugullu H, Zhao JJ (2015) PI3K in cancer: divergent roles of isoforms, modes of activation and therapeutic targeting. Nat Rev Cancer 15:7–24

Van Dort ME, Galbán S, Wang H et al (2015) Dual inhibition of allosteric mitogen-activated protein kinase (MEK) and phosphatidylinositol 3-kinase (PI3K) oncogenic targets with a bifunctional inhibitor. Bioorg Med Chem 23:1386–1394

Wang H, Wu C, Wan S et al (2013) Shikonin attenuates lung cancer cell adhesion to extracellular matrix and metastasis by inhibiting integrin β1 expression and the ERK1/2 signaling pathway. Toxicology 308:104–112

Wang Y, Qu X, Shen HC et al (2015) Predictive and prognostic biomarkers for patients treated with anti-EGFR agents in lung cancer: a systemic review and meta-analysis. Asian Pac J Cancer Prev 16:4759–4768

Wang R, Zhang Q, Peng X et al (2016a) Stellettin B induces G1 arrest, apoptosis and autophagy in human non-small cell lung cancer A549 cells via blocking PI3K/Akt/mTOR pathway. Sci Rep 6:27071

Wang Y, Liu J, Qiu Y et al (2016b) ZSTK474, a specific class Iphosphatidylinositol 3-kinase inhibitor, induces G1 arrest and autophagy in human breast cancer MCF-7 cells. Oncotarget 7:19897–19909

Wang Z, Wang Y, Zhu S et al (2018) DT-13 inhibits proliferation and metastasis of human prostate cancer cells through blocking PI3K/Akt pathway. Front Pharmacol 9:1450

Williams TM, Flecha AR, Keller P et al (2012) Cotargeting MAPK and PI3K signaling with concurrent radiotherapy as a strategy for the treatment of pancreatic cancer. Mol Cancer Ther 11:1193–1202

Wycliffe ND, Grover RS, Kim PD et al (2007) Hypopharyngeal cancer. Top Magn Reson Imaging 18:243–258

Zhang W, Liu HT (2002) MAPK signal pathways in the regulation of cell proliferation in mammalian cells. Cell Res 12:9–18

Zhou Q, Chen Y, Chen X et al (2016) In vitro antileukemia activity of ZSTK474 on K562 and multidrug resistant K562/A02 cells. Int J Biol Sci 12:631–638

Zhou Q, Chen Y, Zhang L et al (2017) Antiproliferative effect of ZSTK474 alone or in combination with chemotherapeutic drugs on HL60 and HL60/ADR cells. Oncotarget 8:39064–39076

Zi D, Zhou ZW, Yang YJ et al (2015) Danusertib induces apoptosis, cell cycle arrest, and autophagy but inhibits epithelial to mesenchymal transition involving PI3K/Akt/mTOR signaling pathway in human ovarian cancer cells. Int J Mol Sci 16:27228–27251